

# A multiscale numerical simulation approach for chloride diffusion and rebar corrosion with compensation model

Xi Tu<sup>\*1</sup>, Zhengliang Li<sup>1</sup>, Airon Chen<sup>2</sup> and Zichao Pan<sup>2</sup>

<sup>1</sup>Key Laboratory of New Technology for Construction of Cities in Mountain Area, Chongqing University, Ministry of Education, 400045 Chongqing, China

<sup>2</sup>Department of Bridge Engineering, Tongji University, 200092 Shanghai, China

(Received August 9, 2017, Revised February 13, 2018, Accepted February 19, 2018)

**Abstract.** Refined analysis depicting mass transportation and physicochemical reaction and reasonable computing load with acceptable DOFs are the two major challenges of numerical simulation for concrete durability. Mesoscopic numerical simulation for chloride diffusion considering binder, aggregate and interfacial transition zone is unable to be expanded to the full structure due to huge number of DOFs. In this paper, a multiscale approach of combining both mesoscopic model including full-graded aggregate and equivalent macroscopic model was introduced. An equivalent conversion of chloride content at the Interfacial Transition Layer (ITL) connecting both models was considered. Feasibility and relative error were discussed by analytical deduction and numerical simulation. Case study clearly showed that larger analysis model in multiscale model expanded the diffusion space of chloride ion and decreased chloride content in front of rebar. Difference for single-scale simulation and multiscale approach was observed. Finally, this paper addressed some worth-noting conclusions about the chloride distribution and rebar corrosion regarding the configuration of rebar placement, rebar diameter, concrete cover and exposure period.

**Keywords:** reinforced concrete structure; chloride diffusion; numerical simulation; mesoscopic; multiscale

## 1. Introduction

Corrosion of steel bar induced by chloride ion from external environment has been recognized as one of the major causes of deterioration of concrete structures, such as infrastructure, bridges and harbors (Roberge 2008). Corrosion of rebar induced by chloride ion could significantly deteriorate the serviceability of the beams (Zhu *et al.* 2016). Corrosion of rebar was divided into two stages. For the first stage, the protective film of rebar was depassivated by chloride ion penetrated from surface of concrete and thus corrosion of rebar initiates once the chloride content on surface of rebar reach a certain thresholding value, defined as critical chloride content (Angst *et al.* 2009, Moodi *et al.* 2014). During this stage, ingress and penetration of chloride within concrete was governed by the diffusion in the pore solution and porosity of concrete, which is generally admitted as the criterion for evaluating service life of Reinforced Concrete (RC) structures (Li and Shao 2014). For the second stage, corrosion of rebar keeps propagating and induces further cracking and spalling due to expansion of rust. Therefore, it is important to accurately assess the diffusion process of chloride ion within concrete, which is meaningful for further evaluation of durability of reinforced concrete structures.

Generally, modeling and analysis for cement-based material were categorized in microscopic scale, mesoscopic

scale and macroscopic scale. On macroscale, concrete was always modeled as homogeneous material. Its material property was determined by the average behavior of all its sub-constituents. On the mesoscale, three phases of heterogeneous space include aggregates, cement and Interfacial Transition Zone (ITZ). On microscale, researcher always treated the constituent consisting of C-S-H and crystalline calcium hydroxide, porosity structures. In fact, macroscopic material behavior of concrete determines structural behavior in higher level and is clearly influenced by the geometry, the spatial arrangement and the material properties of the all material constituents and their mutual interaction, such as cement paste, aggregate and ITZ (Unger and Eckardt 2011).

Nowadays, the macroscopic structural level became gradually inapplicable for structural analysis, design and manufacturing and material models of composites on lower scale attracted more and more attention. Previous study was always limited within single scale. Recently a number of theory research and modelling efforts have been devoted to studying multiscale modeling. Multiscale modeling was usually defined as the integrated numerical process of transferring mechanical and chemical response between lower scale and higher scale (Chen *et al.* 2016, Maekawa *et al.* 2003). A significant advantage of multiscale modeling is optimizing computing loading and enhancing the precision. According to available literature, researchers generally focused on the transferring process of material response between scales.

Multiscale modeling describes the microstructure of ITZ between aggregates and cement pastes and bulk cement paste within mesoscopic model, which comprehensively

\*Corresponding author, Ph.D.  
E-mail: [tuxi@cqu.edu.cn](mailto:tuxi@cqu.edu.cn)

simulates the diffusion of chloride ion considering tortuosity and constrictivity of pore structure (Sun *et al.* 2012). As the major purpose of multiscale modeling to reduce calculation loading, heterogeneous model was always modeled for transferring damage and mass transportation of critical regions from the macroscale to the mesoscale which provided coupling of sub-domains. Damage such as cracks and fatigue is accumulated in concrete composite owing to various types of loading and impact, which propagates to pore and ITZ within concrete between aggregates and cement paste and transforms from lower to structural level (Hiratsuka and Maekawa 2015). For numerical simulation, appropriate element size of multiscale modeling was selected for catering for significant dimension diversity within one model including structural component in over centimeter, cement, aggregate in millimeter and ITZ in micrometer (Guo *et al.* 2012). Besides, some useful indicators were introduced for model adaptation conversing of sub-domains from the macroscale to mesoscale or executing change of meshing size and scale based on concrete image to meet the continuous scale changes of multiscale modeling (Sun *et al.* 2015, Unger and Eckardt 2011). Balance of accuracy and efficiency is the major consideration of multiscale modeling for numerical simulation. The use of homogenous material models in single lower scale leads to extremely large numbers of degrees of freedom, which became challenge for computing hardware (Ladevèze 2004). Designing optimized computational strategies capable of solving such engineering problems is necessary. According to the sample in this paper, total number of nodes and elements of mesoscopic model was much larger than macroscopic model for the same size of analysis space. Computation loading of two-dimensional mesoscopic problem was estimated being over 20 times as macroscopic problem.

Another challenge is success rate of free meshing. As was known, free meshing is much better to simulate actual shape of analysis space and aggregate while background meshing grid is not suitable for small aggregate, irregular boundary and extremely thin interfacial transition zone (Biondini *et al.* 2004, Li *et al.* 2014). However, free meshing for large mesoscopic analysis space is difficult and low success rate of meshing was observed due to irregular arrangement of aggregate. By means of macroscopic model substituting for a part of mesoscopic model, multiscale modeling is able to provide relatively smaller size of mesoscopic model, generate the same filling rate of aggregate and less amount of aggregate, which is no doubt beneficial for raising success rate of meshing.

Due to the significant different size between concrete structures, concrete components, aggregate and interfacial transition zone, a certain small size of element division is guaranteed to ensure appropriate simulation for binder and ITZ, which inevitably results in rather fine meshing density for the entire concrete specimen and thus large amount of nodes and elements for solution. For example, a size of specimen with the side length of 100mm~150mm has been widely adopted for mesoscopic analysis. An estimated of amount for elements is always around  $10^4$  for two-dimensional and  $10^6$  for three-dimensional. Accordingly, respective time consumption becomes

uncontrollable for large amount of batch calculation even sparse matrix solution included.

In mesoscopic view, concrete is the composite of binder, aggregate, void and interfacial transition zone (ITZ), a hypothesized fine layer located between aggregate and binder. For mesoscopic numerical simulation, cement was considered as the diffusion media for chloride ion due to its porosity structure and water filling. For most numerical simulation, distribution of aggregate was randomly generated regarding gradation. Generally, Fick's second law is the generally adopted description for simulating the diffusion of chloride within solution. In concrete, the calculated diffusion process of chloride was improved considering the effective connected pore, humidity, binding of concrete and other factors (Ye *et al.* 2016).

Though clear model for reinforcement corrosion and environmental attack still has not been widely accepted, researchers devoted efforts on laboratorial research by means of natural experiments (Francois and Arliguie 1999, Vidal *et al.* 2004, Vidal *et al.* 2007, Zhang *et al.* 2009, Zhang *et al.* 2010) and accelerated experiments (Andrade *et al.* 1993, Chun Qing 2000, Liu and Weyers 1998, Pritpal and Mahmoud 1999, Torres-Acosta *et al.* 2007, Torres-Acosta Andrés and Mart'inez-Madrid 2003) about the process of chloride diffusion and corrosion. Based on currently available experimental data, most previous works focused on the experimental phenomena and outcome of corrosion and clear deterministic analysis model has been summarized. On the other hand, approximate law of corrosion has become more and clearer till now and thus a simplified evaluation method is more practical. Biondini (2006) introduced a reasonable linear damage model for corrosion of rebar under aggressive agent, which evaluates corrosion rate according to the real-time chloride content surrounding rebar. Despite of the unclear principle of corrosion, based on the natural damage mode of corrosion, this linear damage model can provide the approximate law of damage process.

This paper addressed two important aspects regarding multiscale modeling for numerical simulation of chloride ion diffusing within concrete. Firstly, a comprehensive multiscale approach combining both mesoscale and macroscale connected by Interfacial Transition Layer was introduced and its feasibility was discussed by means of analytical deduction and numerical simulation. Secondly, with the introduced numerical tools, characteristics of diffusion of chloride ion in corner and straight edge of concrete were studied by means of numerical simulation. Their induced corrosion of rebar was also calculated to study the time evolution of corrosion process. Besides, in order to study the diffusion process of chloride within concrete, this paper summarized and described the two-dimensional approach for simulating the diffusion process of chloride from surface of concrete based on modified Fick's law and evaluating the corrosion process of rebar induced by chloride considering cement hydration, temperature and concrete resistance.

## 2. Multiscale modeling and simulation

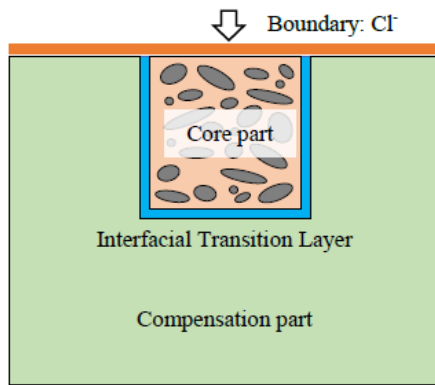


Fig. 1 Two-dimensional multiscale model with Core part and Compensation part for simulating chloride diffusion within concrete

### 2.1 Multiscale modeling

In mesoscopic numerical simulation for chloride diffusion, usually 100–200 mm size of specimen in square or rectangle was considered. Within this typical size of analysis space, enough number of aggregates with various size were included for in-depth study. Within limited analysis space, chloride ion would be able to penetrate and saturate the whole space within the assessing period, as was shown in Fig. 10, which indicated the whole space was inadequate for further simulation. However, it would be impossible to increase the size of analysis space due to two reasons. First, several times of original size of analysis space will generate much more nodes and elements, especially for three-dimensional problem. Second, to control computing loading, changing the grading curve and ignoring fine aggregate will cause inaccuracy of numerical simulation.

In this paper, a scheme of multiscale modeling was introduced in terms of balancing amount of nodes and elements and calculation accuracy (Fig. 1). In the view of multiscale modeling, based on original mesoscopic model including multi-phase components which was defined as Core part, a macroscopic compensation model, which was defined as Compensation part, was modeled. The aim of introducing compensation part was creating addition space to absorb the chloride within core part and adjusting the distribution of chloride content within core part, which means redistribution of chloride in larger space.

Due to different definition of nodal chloride content and diffusion coefficient in mesoscopic model and macroscopic model, the two types of models cannot be directly combined and analyzed simultaneously. In this paper, Interfacial Transition Layer (ITL) was introduced to connect both models at the interface which consists of a group of nodes and elements, shown in Fig. 1. ITL was designed as a banded shape transition zone allowing chloride ion diffusing from core part into compensation part. Within each time step, core part and compensation part were analyzed sequentially and the chloride content at interface of the two parts was transferred based on the function of ITL.

It is worth noting that, the most important precondition

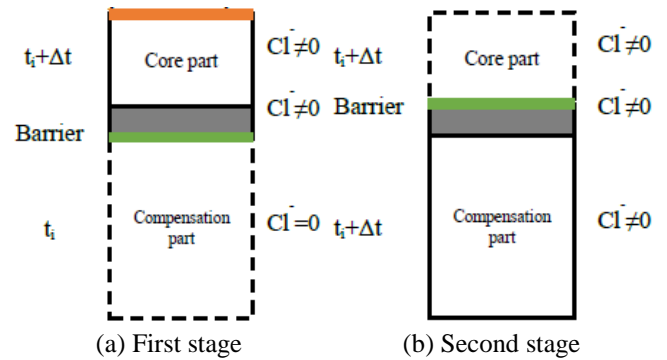


Fig. 2 The two stages of chloride diffusion at interfacial transition layer connecting macroscopic and mesoscopic model

is the mechanism of ITL for transporting the chloride ion, which generating equivalent diffusion and distribution of chloride within the model on the same scale. ITL could be composed by a row of common nodes occupied by both mesoscopic model and macroscopic model, as well as an amount of elements with certain thickness stuck by both models.

The process of transferring chloride ion within ITL in one-dimension was illustrated in Fig. 2. For initial state, Analysis space of three phases including core part, compensation part and ITL was modeled respectively. Boundary condition was set at surface of concrete, which was the top of core part shown in Fig. 2.

This mixed model behaved in sequential multiscale process. For the mixed case that core part is in mesoscale and compensation part in macroscale, equivalent chloride content in ITL will be calculated and transferred. Definitions of chloride content in both parts were different. Chloride content in macroscopic model was measured in concrete and the value in mesoscopic model was measured in cement. Therefore, a necessary procedure was included that the value of chloride content in ITL should be calculated for each stage. Simulation of chloride diffusion within mixed model was divided into two stages of diffusion and two steps of conversion.

#### 1) The first stage of diffusion

Core part and ITL were connected as common interface while ITL and compensation part were disconnected. With one time-step, chloride ion penetrated into core part from boundary condition. During current stage, diffusion of chloride ion restrained within core part and ITL. The chloride content of core part and ITL rose up from previous content while compensation part kept unchanged.

#### 2) Conversion from mesoscale to macroscale within ITL

The simulated result in region in core part covered by ITL was converted from mesoscale to macroscale within this step. For the instance of center bottom of concrete boundary, compensation part was modeled as simply one-dimensional model. Within core part, elements with their centroid included in Interfacial Transfer Layer were identified (the region enclosed by red dashed line in Fig. 3). Weighted mean value of chloride content of these involved

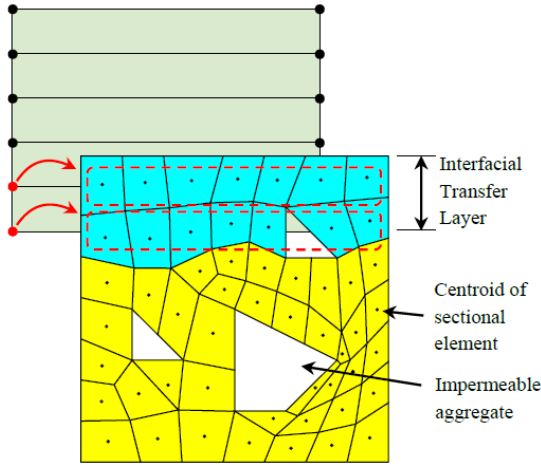


Fig. 3 First step of conversion: calculation nodal chloride content of compensation part from involved elements in core part (Red dashed: Coverage of nodes in compensation part; Blue: Involved elements in core part; Yellow: Uninvolved elements)

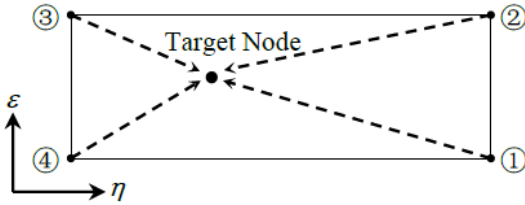


Fig. 4 Second step of conversion: interpolating chloride content at target node based on four nodal value

elements was calculated for the nodal value of ITL in macroscale.

### 3) The second stage of diffusion

A new barrier was inserted at common border of core part and ITL which was equal to cut down the connection of these parts. The existing barrier at common border of compensation part and ITL was removed. During this stage, chloride redistributes within the region including ITL and compensation part.

### 4) Conversion from macroscale to mesoscale within ITL

As the inverse process of the 2nd step, the nodal content of mesoscopic core part was interpolated from macroscopic compensation part in the form of regular rectangle element. As was illustrated in Fig. 4, the outer rectangle represents the uniform quadrilateral model in compensation part and the target node denotes the node included within core part. Four nodes of the quadrilateral were numbered in counterclockwise.

Regarding arbitrary coordinate of target node, its value,  $\phi_t$ , was the interpolation of the values at four vertices. For linear Lagrange shape function, the value of target node was expressed as below

$$\phi_t = \frac{1}{4} \sum_{i=1-4} (1 + \varepsilon_i \varepsilon_i)(1 + \eta_i \eta_i) \phi_i \quad (1)$$

Here,  $\varepsilon_i$  and  $\eta_i$  are the natural coordinate for the target

node. Moreover, with known position of target node in global coordinate system,  $(x_t, y_t)$ , the coordinate interpolation was expressed in the following form

$$\begin{cases} x_t = \frac{1}{4} \sum_{i=1-4} (1 + \varepsilon_i \varepsilon_i)(1 + \eta_i \eta_i) x_i \\ y_t = \frac{1}{4} \sum_{i=1-4} (1 + \varepsilon_i \varepsilon_i)(1 + \eta_i \eta_i) y_i \end{cases} \quad (2)$$

Thus, with least square method, the approximate of  $\varepsilon_i$  and  $\eta_i$  were solved by (2) and accordingly  $\phi_i$  was calculated by (1).

## 2.2 Analytical solution for finite space with exposed and time-dependent boundary

In following section, this paper discussed about the feasibility of multiscale model in analytical approach. Due to the sectional design of rebar in concrete member, some research on chloride diffusion were transformed within two-dimensional space equivalently. For the case on center of bottom of concrete section, concrete and outer atmosphere were divided into two infinite half-space into which the boundary plane divides the three-dimensional space. Regarding numerical simulation, for the same configuration of boundary condition and diffusivity of concrete, all points in concrete at the same depth from the boundary behave in the same characteristics of diffusion. In simplification, the chloride diffusion in three-dimensional and two-dimensional space were equivalent to one-dimensional one. Therefore, the problem was simplified to one-dimensional macroscopic model and the analytical solution for finite space with both exposed and sealing boundary was discussed. Usually diffusion of chloride within solution was expressed by linear Fick's second Law

$$\partial C / \partial t = D \cdot \nabla^2 C \quad (3)$$

Where,  $D$  is the diffusion coefficient of concrete.  $C$  denotes the chloride content. Considering the boundary condition of  $C(0, t) = C_s$  and  $C(\infty, t) = C_0$ . As was widely known, according to Laplace transform, the analytical solution of above partially derivative equation was

$$C(x, t) = C_0 + (C_s - C_0) \left[ 1 - \operatorname{erf} \left( x / 2\sqrt{Dt} \right) \right] \quad (4)$$

Where,  $\operatorname{erf}$  is Gauss error function. The limitation of the above solution is the premise of infinite space for boundary condition, which is suitable for concrete members with large thickness compared with thickness of concrete cover, but inaccurate for typical beams and slabs. For finite space, three-dimensional analytical solution by means of Separation of variables was discussed and deduced by Li (Li *et al.* 2009). For one-dimensional space, assuming the total length of diffusion space is  $l$ .  $x$  axis is the longitudinal direction of the one-dimensional model. Initial condition for diffusion space,  $C(x, 0) = C_0$  and boundary condition, exposed boundary:  $C(\Gamma_1, t) = C_s$ ; sealing boundary:  $\partial C / \partial x|_{\Gamma_2} = 0$ , were all considered. The schematic illustration was shown in Fig. 5.

The simplified function of chloride content including the

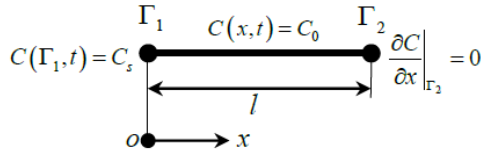


Fig. 5 Analysis model for analytical deduction

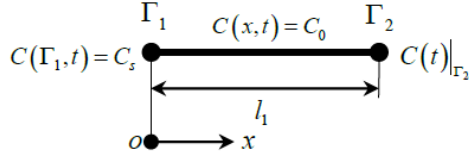


Fig. 6 Illustration of core model for diffusion with compensation

variables of time and depth in one-dimensional space according to Li's solution was expressed as followed

$$C = C_s + (C_0 - C_s) \sum_{n=1}^{\infty} \frac{4}{(2n-1)\pi} \sin\left(\frac{2n-1}{2l}\pi x\right) e^{-D\left(\frac{2n-1}{2l}\pi\right)^2 t} \quad (5)$$

If zero chloride content for initial condition,  $C_0=0$ , was considered, (5) was simplified below

$$C = C_s \left[ 1 - \sum_{n=1}^{\infty} \frac{4}{(2n-1)\pi} \sin\left(\frac{2n-1}{2l}\pi x\right) e^{-D\left(\frac{2n-1}{2l}\pi\right)^2 t} \right] \quad (6)$$

The aim of following section was to deduce the expression of analytical solution of chloride content with both exposed boundary and time-dependent boundary according to Li's deduction process and prove that the development in core model with predefined time-dependent boundary condition is same as the part in full model. For the consideration of compensation for chloride diffusion, a part of the full model was extracted and called as **Core Model**. The schematic illustration of core model was shown in Fig. 6. The length of core model was  $l_1$  while assuming the length of full model was  $l_2 (l_2 > l_1)$ .

Being different with the precondition of Li's solution (Li *et al.* 2009), the boundary condition  $\Gamma_2$  of core model was modified into the function of time-dependent boundary  $\Gamma_2'$  strictly defined by (6) set at  $l_1$ , expressed in (7). The other parameters and definition were the same as before. For simplification, zero chloride content for initial condition,  $C_0=0$ , was considered.

$$C(t)|_{\Gamma_2} = C_s \left[ 1 - \sum_{n=1}^{\infty} \frac{4}{(2n-1)\pi} \sin\left(\frac{2n-1}{2l_2}\pi l_1\right) e^{-D\left(\frac{2n-1}{2l_2}\pi\right)^2 t} \right] \quad (7)$$

Considering a temporary variable,  $V$ .

$$V = C - C_s \quad (8)$$

Apart initial condition and boundary condition, the time-dependent boundary  $\Gamma_2'$  was expressed as

$$V|_{x=l_1} = -C_s \sum_{n=1}^{\infty} \frac{4}{(2n-1)\pi} \sin\left(\frac{2n-1}{2l_2}\pi l_1\right) e^{-D\left(\frac{2n-1}{2l_2}\pi\right)^2 t} \quad (9)$$

By means of Separation of variables,  $V$  was expressed as

$$V(x, t) = X(x) \cdot T(t) \quad (10)$$

By introducing boundary condition of exposed surface  $\Gamma_1$ , the general solution of  $X$  was simplified as

$$X(x) = B \sin(\alpha x) \quad (11)$$

For time-dependent boundary  $\Gamma_2'$ , combining (9) and (11), we obtained the expression of  $\alpha$

$$\alpha_n = \frac{2n-1}{2l_2} \pi \quad (n=1, 2, \dots) \quad (12)$$

Thus particular solution of  $X$  was:

$$X_n(x) = k_n \sin\left(\frac{2n-1}{2l_2} \pi x\right) \quad (13)$$

The particular solution of  $T$  was solved as

$$T_n = -d_n e^{-D\alpha_n^2 t} \quad (14)$$

Thus general solution of  $V$  was

$$V_n = e_n \sin\left(\frac{2n-1}{2l_2} \pi x\right) e^{-D\alpha_n^2 t} \quad (15)$$

Where,  $e_n$  was the  $n$ th order of unknown expression and  $e_n = k_n \cdot d_n$ . Considering initial condition ( $t=0$ ), we obtained from (15)

$$\sum_{n=1}^{\infty} e_n \sin\left(\frac{2n-1}{2l_2} \pi x\right) = -C_s \quad (16)$$

Due to Orthogonality of the following function series

$$\int_0^{l_1} \sin(\alpha_m x) \sin(\alpha_n x) dx = \begin{cases} 0 & m \neq n \\ l/2 & m = n \end{cases} \quad (17)$$

Combining (16) and (17), we obtained

$$e_n = -\frac{4C_s}{(2n-1)\pi} \quad (18)$$

Combine (8), (15) and (18), finally we obtained

$$C = C_s \left[ 1 - \sum_{n=1}^{\infty} \frac{4}{(2n-1)\pi} \sin\left(\frac{2n-1}{2l_2} \pi x\right) e^{-D\left(\frac{2n-1}{2l_2}\pi\right)^2 t} \right] \quad (x \in [0, l_1]) \quad (19)$$

Therefore, even considering the time-dependent boundary, the development of diffusion within core model was exactly the same as the original model, which proved the feasibility of compensation for chloride diffusion.

### 2.3 Comparison based on numerical simulation

Numerical simulations were performed with the computer coding program based on finite difference method in order to study the transferring process of chloride ion within the three-phase model with ITL and the error

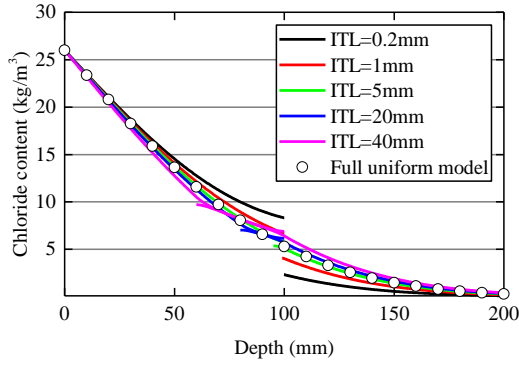


Fig. 7 Chloride content profile for different ITL thickness, 100mm size of specimen at 100a

compared with uniform heterogeneous model. For the view of comparison, one-dimensional model configuration was described as below, which was equally meshed into 500 elements for core part and 1000 elements for compensation part. The effective diffusion coefficient  $D_e$  was  $1.0 \times 10^{-12}$  m<sup>2</sup>/s. 26 kg/m<sup>3</sup> of chloride ion concentration solutions was considered for surface conditions in the calculations. The boundary condition used for the numerical simulation was expressed as

$$\begin{cases} C_f = C_s & x = 0 \\ C_f = C_0 & x \neq 0 \end{cases} \quad (20)$$

Where  $C_0$  is the chloride content present in the pore solution before the exposure to a salt solution for concrete (kg/m<sup>3</sup> of pore solution). In the following numerical simulation,  $C_0=0$  was assumed.  $C_s$  is the chloride content of the salt solution on the outer surface (kg/m<sup>3</sup> of solution). Nonlinear binding was neglected. Cases with different thickness of ITL were analyzed.

Fig. 7 showed the chloride content profile of the thickness of ITL from 0.2 mm-40 mm for the core part in 100mm total length. The data in scatter round point indicated the full-length uniform model which was the control data for the other cases. Result revealed small thickness of ITL became ineffective compensating the core part while similar phenomenon was observed in the case with over 20 mm of ITL. Apparently an applicable thickness of ITL was about to be analyzed. Fig. 8 showed the error profile of ITL thickness. The cases with the length of core part from 80 mm to 200 mm were discussed. The maximum relative error compared with full-length uniform model from boundary condition to the point 20 mm away from end of core part were summarized. Result showed the thickness around 9.25 mm for ITL was a reasonable value for compensation which is the valuable base for further numerical simulation. Based on this configuration, relative error for main part of core model could be limited within 0.1%.

### 3. Assessing approach

#### 3.1 Diffusion model of chloride

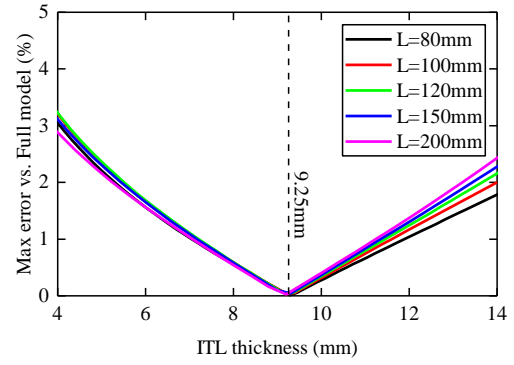


Fig. 8 Max error of core part vs. ITL thickness for five types of specimens at 100a (L denotes the length of core part)

Transportation of chloride ion in porous medium such as cementitious materials is mainly a diffusive phenomenon due to concentration gradients (Maekawa *et al.* 2009). The diffusion of chloride ion within concrete components was admitted as a complex process, which was influenced by many factors including water/cement ratio, porosity of cement, additive, aggregate, temperature, humidity, environmental chloride content, binding effect of binder, hydration of cement. The above process could be simulated by numerical approach based on available environmental attacking condition and material properties. Fick's second law was widely adopted as the expression of principle differential equation (Yuan *et al.* 2009)

$$\omega_e \frac{\partial C_f}{\partial t} = \frac{\partial}{\partial x} D_e \omega_e \frac{\partial C_f}{\partial x} - \frac{\partial C_b}{\partial t} \quad (21)$$

$$C_t = C_b + C_f \cdot \omega_e \quad (22)$$

Where,  $C_f$  is the free chloride content (in kg/m<sup>3</sup> of solution);  $C_b$  is the bound chloride content (in kg/m<sup>3</sup> of concrete);  $C_t$  is the total chloride content (in kg/m<sup>3</sup> of concrete);  $D_e$  is the effective diffusivity;  $\omega_e$  is the evaporable water content (in volume percentage of concrete). Considering complexity of cross sections of bridge pier, appropriate preliminary division and meshing grid are processed by means of some meshing tools or commercial FE software. Experimental data indicated that due to cement hydration and chloride content, the chloride diffusion coefficient is strongly dependent on the exposure period of concrete (Mangat and Molloy 1994).

#### 3.2 Corrosion model of rebar

Corrosion of rebar initiates in the form of galvanic reaction between Ferrous and oxygen accelerated by the presence of active free chloride ion once the protection of high pH (>12.5) hydration products was depassivated. Corrosion continues with the cycle of electric current between cathode and anode, which was influenced by high chloride concentration at the level of the rebar, environmental temperature, electrical resistivity of concrete and hydration of cement. The corrosion model regressed by Liu (Liu and Weyers 1998) based on experimental data

included the influence of chloride content, temperature, concrete cover resistance and time of cement hydration, which was expressed as

$$\ln(1.08i_{corr}) = 8.37 + 0.618 \cdot \ln(1.69Cl) - 3034/T - 0.000105R_c + 2.32t^{-0.215} \quad (23)$$

Where,  $i_{corr}$  is corrosion current intensity ( $\mu A/cm^2$ );  $Cl$  is chloride content ( $kg/m^3$ ), which was obtained from numerical simulation result of chloride diffusion;  $T$  is temperature at the depth of steel surface (in degree Kelvin);  $R_c$  is the resistance of the cover concrete (ohms);  $t$  is corrosion time duration (years). With the data chloride content obtained by numerical simulation and the other parameters assumed previously, the real-time corrosion current rate at each time step of numerical simulation was calculated by (23). Thus the corrosion depth on surface of rebar was calculated as (Šavija *et al.* 2013)

$$D_{t+\Delta t} = D_t - 0.023 \cdot i_{corr} \Delta t \quad (24)$$

Where,  $D_t$  is remaining rebar diameter (mm) at  $t$  years, here 20mm adopted;  $D_{t+\Delta t}$  is reduced rebar diameter (mm) at  $t+\Delta t$  years;  $\Delta D|_{\Delta t}$  is reduction of rebar diameter (mm) for the period of propagation for the duration time of  $\Delta t$  years.

#### 4. Numerical simulation for diffusion of chloride including compensation

##### 4.1 Diffusion properties of environment and concrete regressed by least square method

Diffusion coefficient and boundary condition of chloride ion are the major parameters for numerical simulation, which are generally determined by environmental condition and concrete. Most concrete structures and bridges attacked by penetration of chloride ion in eastern coastal region of China are in danger of deterioration of durability, which was the major concern of this paper.

In order to obtain the essential parameters for further analysis, generally it is accomplished by least square regression method based on analytical solution of Fick's second law. Zhao (Zhao *et al.* 2009) investigated a reinforced concrete pier located in eastern coastal region of China for in-site measured data of chloride content. The best matched apparent surface chloride content is 0.708 (%  $w_c$ ) and apparent chloride diffusivity is  $1.837 \times 10^{-12} m^2/s$ .

##### 4.2 Comparison for compensation approach

The compensation for mesoscopic model was discussed by means of numerical simulation in this section. Four types of model were developed, including mixed model, full mesoscopic model, core mesoscopic model and full macroscopic model. In order to testify the accuracy of mixed model, the other three models were analyzed. In these four types of models:

- **Mixed model** was developed according to the approach introduced in this paper. In this model, for the aim of balancing accuracy and time consumption, a  $100 \times 100$  mm square (Fig. 9(c)) and a  $100 \times 200$  mm

rectangle (Fig. 9(b)) were considered for two-dimensional core mesoscopic model including aggregate and one-dimensional compensation macroscopic model respectively, which was equivalent 1:2 compensation ratio. Besides, for the aim of compensation, an overlapped area occupied by both models with a certain thickness while its width kept the same as the core model was considered as ITL. Chloride ion was exchanged within ITL for both models. The boundary condition was set at the bottom edge of core model shown in Fig. 10.

- For the aim of comparison, a  $100 \times 300$  mm rectangle **Full mesoscopic model** was developed in order to obtain the diffusion of chloride ion, which was considered as the correct result (Fig. 9(a)). Aggregates were generated according to the aggregate grading curve. Boundary condition was set as the same as mixed model.

- **Core mesoscopic model** was based on a  $100 \times 100$  mm square, which was the same as the core model in mixed model (Fig. 9(c)). The distribution of chloride content within core mesoscopic model was considered as the uncompensated case compared with mixed model for the aim of investigating error of uncompensated cases. Configuration of boundary condition was the same as mixed model.

- **Full macroscopic model** was the simplest model with least nodes and elements and expectantly the least time consumption. This model was simplified as one-dimensional model with the similar configuration of boundary condition as mixed model.

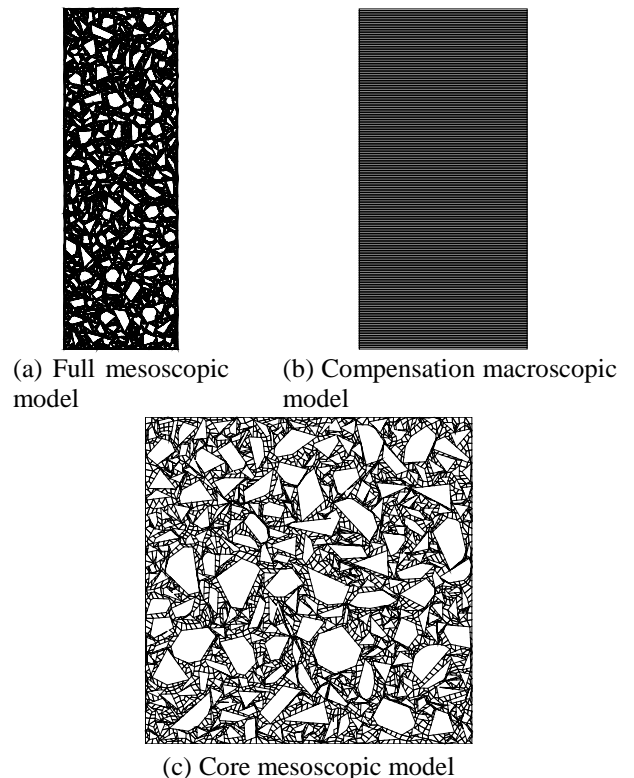


Fig. 9 Style and characteristic dimension of the elements of FE model

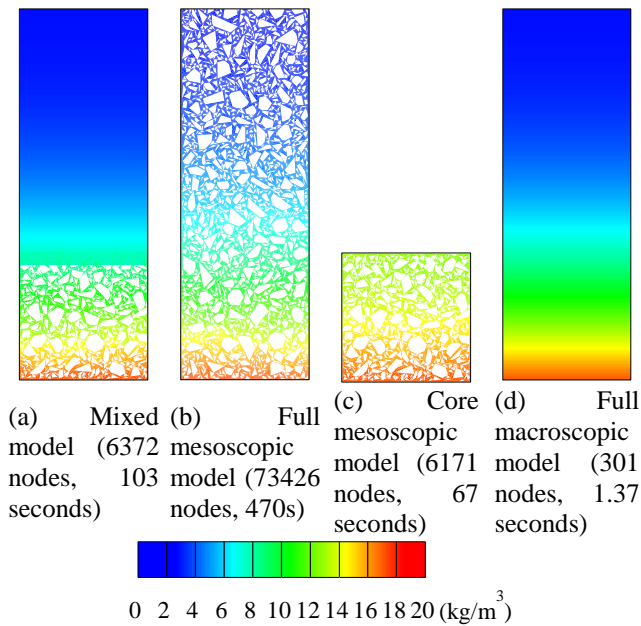


Fig. 10 Contour of chloride content for four types of models and corresponding time consumption, 100a

Due to mesoscopic configuration of core model in compensation case, zone of ITL was vertically divided into several uniform thickness layers. During transferring chloride beyond scales, mean chloride content of each layer of mesoscopic model was calculated and assigned to the covered element in macroscopic model. On the contrary, nodal chloride content in mesoscopic model was obtained by interpolation in macroscopic model regarding the nodal coordinate.

All four types of models were considered as the same material properties and initial parameters. 55% filling percentage of aggregate for mesoscopic model was considered. Boundary condition and diffusion coefficient were set as the value obtained in previous section. Equivalent diffusion coefficient for mesoscopic model was calculated regarding the distribution of effective aggregate gradation of mesoscopic model. Binding of chloride ion was neglected. A total 100 years of exposure period was analyzed. Fig. 10 presented the distribution of chloride content by numerical simulation from all four models. White polygon blocks within the figures indicated the random generated aggregate occupying the diffusion space. Contour of chloride content showed the similar distribution within the range of core part for all four cases but slight difference color was found in core mesoscopic model compared with the other three cases, which proved the effect of compensation approach. Time consumption of various approaches were listed in Fig. 10 based on the author's computer hardware configuration. Accordingly, mixed model provided optimized total number of DOFs compared with full mesoscopic model and was able to describe detail distribution of chloride content around rebar in further study compared with full macroscopic model.

Fig. 11 indicated the comparison of results from the specimen investigated exposed in coastal environment for 51 months by numerical simulation and in-site

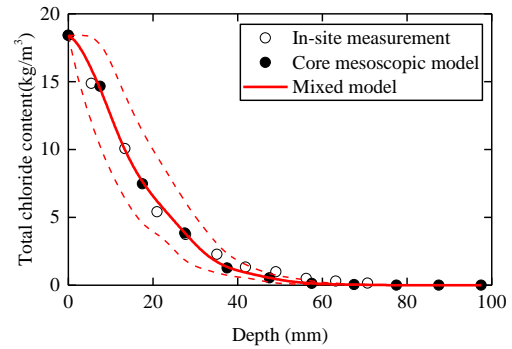


Fig. 11 Comparison of profile and envelop of chloride content at 51 months, 10 mm ITL

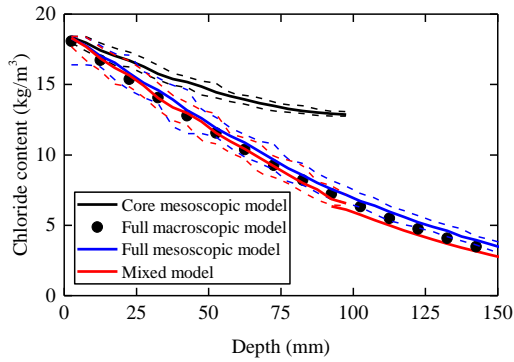
measurement. According to the obtained diagram, the result from numerical simulation agreed well with in-site measurement, which can conclude the numerical approach is practical. It is worth noting that there was no significant difference between mixed model and core mesoscopic model. The reason is for short exposure period, limited distribution of chloride within analysis space suppressed the effect of compensation which was useful for long period of numerical simulation.

Fig. 12(a) indicated the profile of horizontal mean chloride content along depth with the chloride content distribution shown in Fig. 10. Dashed lines drawn in Fig. 12(a) denoted the maximum and minimum values corresponding to the solid line in the same color. The difference of diagrams between mixed model and core mesoscopic model proved effectiveness of the compensation approach introduced in this paper. For example, at the depth of 50mm which is the distance from common front of rebar to surface of concrete, mean chloride content decreased over 18.4% at 100 years of exposure once taking consideration of compensation. On the other hand, mean chloride content in mixed model was closed to the result from full macroscopic model. The result from full mesoscopic model was neglected for the reason that the random distribution of aggregate caused inevitable indeterminate result, which was difficult for further recognition.

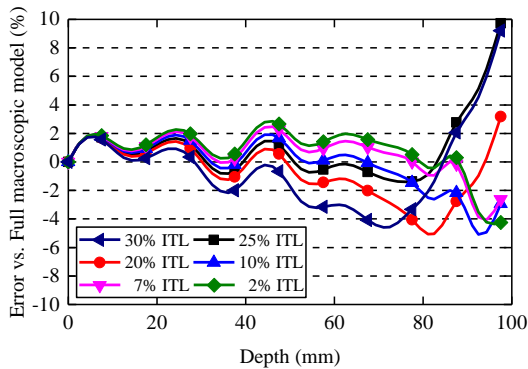
Fig. 12(b) indicated the error of mean chloride content of mixed model compared with full macroscopic model considering various overlapping percentage of ITL. As was shown, for all cases within 10%-25% overlapping, error was constrained within the range of  $\pm 2\%$  for the depth no more than 60 mm. however, beyond this depth, error increased and became uncontrollable within the range of ITL. In this case, 20% overlapping was an appropriate configuration for ITL.

#### 4.3 Statistical assessment of chloride diffusion and rebar corrosion

For mesoscopic numerical simulation, distribution of aggregate was recognized as the major influence factor for development of chloride (Pan *et al.* 2015). Chloride content on surface of rebar significantly varied with different arrangement and grading of aggregate. Thus both mean and



(a) Profile and envelop of chloride content at 100a, 10 mm ITL (Dashed denotes maximum and minimum limits)



(b) Relative error of Mixed model vs. Full macroscopic model for thickness of ITL from 2% to 30%

Fig. 12 Comparison of profiles of chloride content regarding compensation and corresponding error from numerical simulation, 100mm size of specimen assessed

Table 1 Details of model comparison for concrete cover thickness and rebar diameter regarding chloride diffusion and rebar corrosion

Cover thickness, $C$ (mm)	Rebar diameter, $D$ (mm)				
	12	16	20	25	28
20		×			
30		×			
40		×			
50	×	×	×	×	×
60		×			

maximum distribution of chloride ion in terms of random aggregate models became the major consideration.

In this section, chloride content on the front of rebar in terms of the configuration was studied by the multiscale numerical simulation introduced previously. According to general engineering design, a group of concrete cover thicknesses and rebar diameters were devised for detailed comparison of chloride diffusion and rebar corrosion, shown in Table 1. For the purpose of comparison, rebar in diameter of 16 mm was selected for the cases in different cover thickness and 50 mm cover thickness for the comparison of rebar diameters. By means of the random aggregate generation approach and considering reasonable computing loading, 100 two-dimensional samples for each combination of concrete cover thickness and rebar diameter

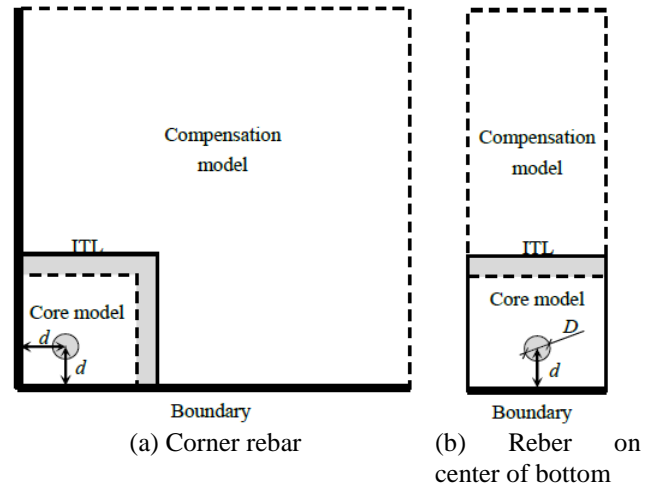


Fig. 13 Geometrical configuration of analysis space and rebar (Solid: core model; Dashed: compensation model; Bold: boundary condition; Gray: ITL; Circle: rebar)

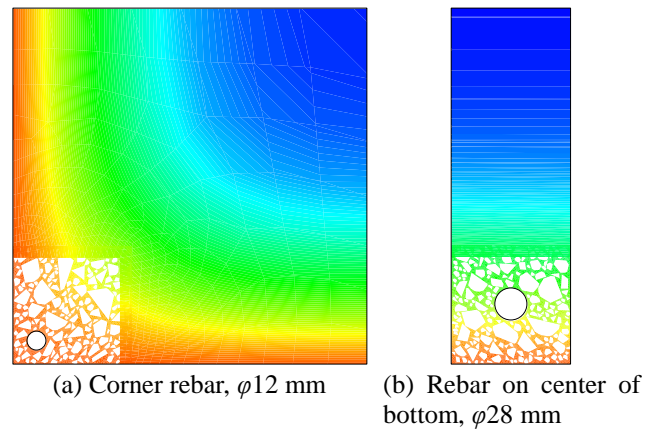


Fig. 14 Two-dimensional typical distribution of aggregate and chloride content with compensation, 100a

was modeled considering random distribution of aggregate. It also justified to a certain extent that interfacial transition zone was neglected for all following cases for simplification.

Besides, two common placements of rebar including right angle corner and straight edge were considered. Rebar placed in the corner of concrete section (Fig. 13(a)) and placed in the center of bottom side of concrete section (Fig. 13(b)) listed in Table 1 were tested. Term  $d$  denotes the cover thickness and the diameter,  $D$ , of circle refers to diameter of rebar. A two-dimensional mesoscopic core model in the size of 100×100 mm was created. In order to guarantee the effect of compensation, total size of compensation model was designed as two times of core model. 10 mm thickness of ITL was considered for compensation process. Fig. 14 showed typical distribution of chloride content within core mesoscopic model and compensated macroscopic model at 100 years of exposure period for both cases of rebar placed in corner and center of bottom. The contour clearly described sound transition of chloride content near ITL on both cases and proved the effect of compensation as well.

The circle curve of rebar was meshed into a series of

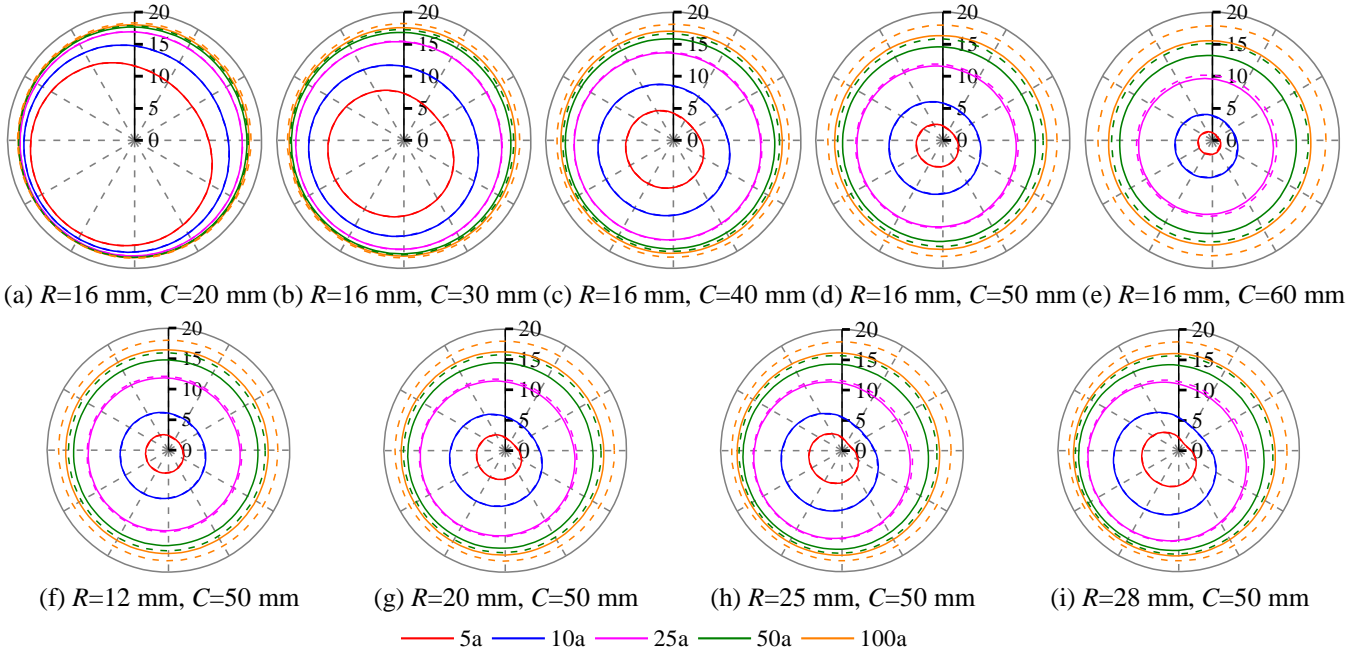


Fig. 15 Polar distribution of chloride content on cross section of corner rebar for two cases: compensated (solid) and uncompensated (dashed)

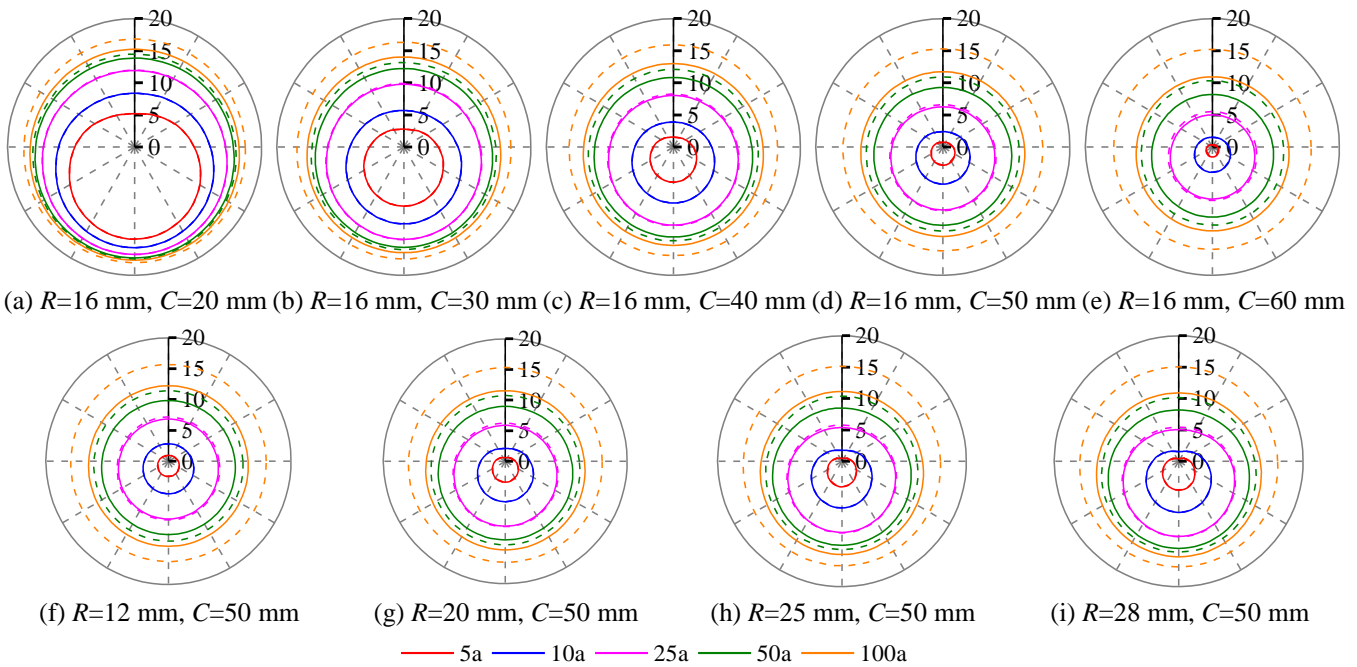
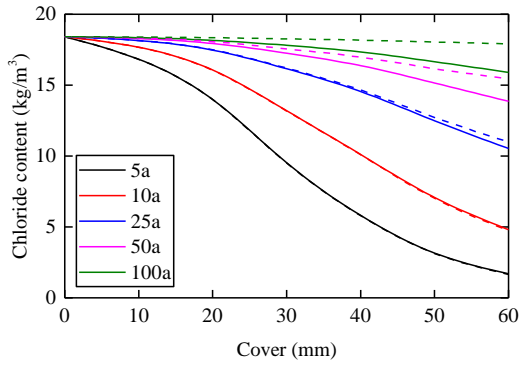


Fig. 16 Polar distribution of chloride content on cross section of rebar on center of bottom side for two cases: compensated (solid) and uncompensated (dashed)

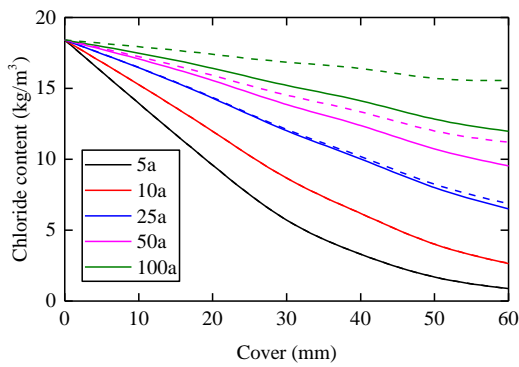
node and nodal chloride content was obtained from result of FE analysis. For all 100 samples of each research case, mean value of chloride content on each nodes around rebar was calculated and plotted in polar coordinate. Fig. 15 and Fig. 16 showed the polar distribution of mean chloride content on cross section of rebar for both cases whether compensation model was considered. Depending on the exposure period, chloride content were plotted in different colours, shown in legend on the bottom. For the cases of corner rebar, distribution of chloride content developed

towards lower-left, which matched the configuration of boundary condition. Similar distribution was observed for the rebar on center of bottom.

Mean chloride content vs. cover thickness for 16 mm rebar and mean chloride content vs. diameter for 50 mm cover were summarized in Fig. 17 and Fig. 18 respectively. Due to different configuration of boundary condition, mean chloride content around corner rebar developed more than rebar on center of bottom side. An obvious result showed lower chloride content in compensation case since solid

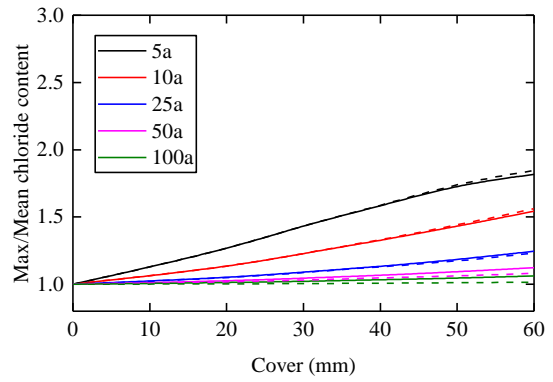


(a) Corner rebar

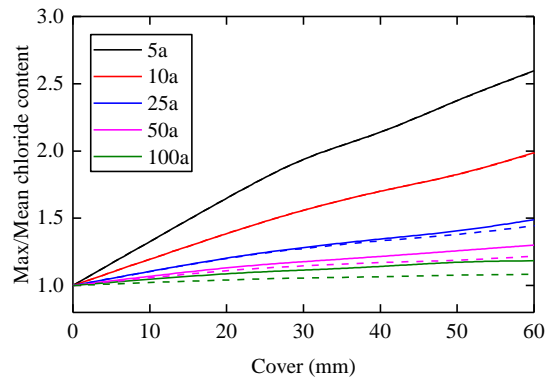


(b) Rebar on center of bottom side

Fig. 17 Mean chloride content vs. cover thickness, 16mm diameter rebar. (Solid-with compensation; Dashed-without compensation)

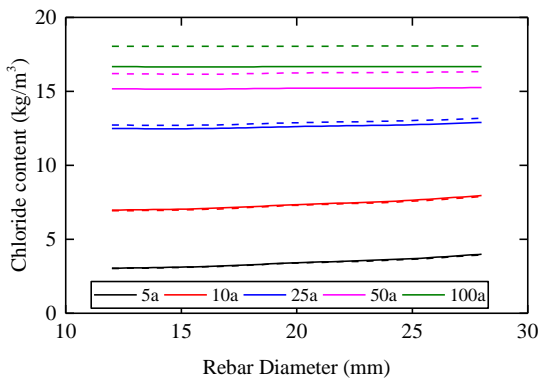


(a) Corner rebar

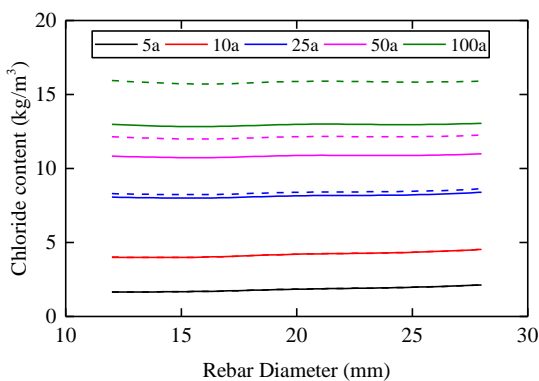


(b) Rebar on center of bottom side

Fig. 19 Comparison of maximum chloride content to mean value, 16 mm diameter rebar. (Solid-with compensation; Dashed-without compensation)



(a) Corner rebar



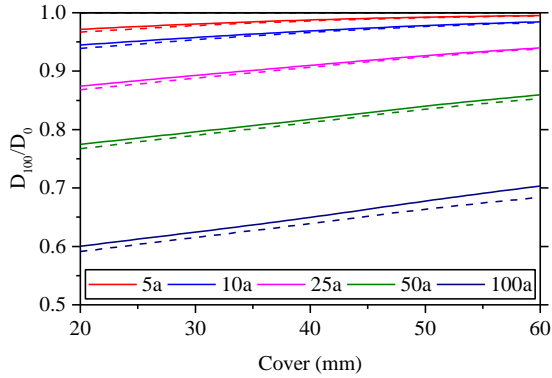
(b) Rebar on center of bottom side

Fig. 18 Mean chloride content vs. diameter, 50mm cover. (Solid-with compensation; Dashed-without compensation)

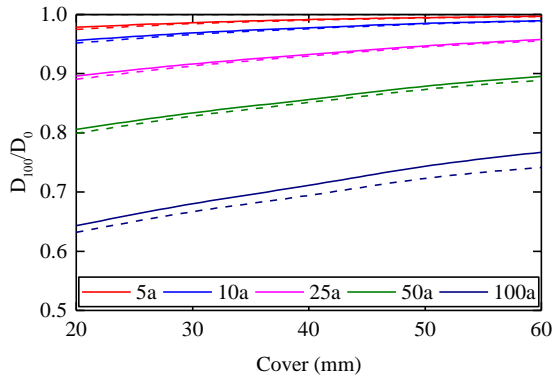
lines were all under corresponding dashed lines in the figures, which attributed the larger diffusion space in compensation cases.

Another important statistical parameter is the maximum chloride content. Fig. 19 indicated the ratio of maximum chloride content vs. mean value. It is worth noting that, for limited smaller space, mean chloride content raised more than the compensated case and thus the max/mean ratio was reduced, which was observed as the relationship between dashed line and solid line in Fig. 19. Besides, for thicker concrete cover, indeterminate of diffusion of chloride was enhanced by the grid of aggregate and Max/Mean ratio increased with concrete cover. The major influence of compensation was concluded as the time of exposure. For longer time, such as 100a (green line), solid line (compensation) was significantly higher than dashed (without compensation). For larger diffusion space, chloride content around surface of rebar did not attain enough saturation, meaning lower mean value, which resulted in higher Max/Mean ratio. But for early stage of diffusion, such as 5a (black line), the core part has not been fully saturated by chloride ion and thus both solid line and dashed line coincided.

Corrosion of rebar based on previous data of chloride content was discussed in the following section. Since Liu summarized the corrosion model by means of 3LP devices, the corrosion current provided by (23) only represents the overall corrosion process of rebar and cannot describe



(a) Corner rebar

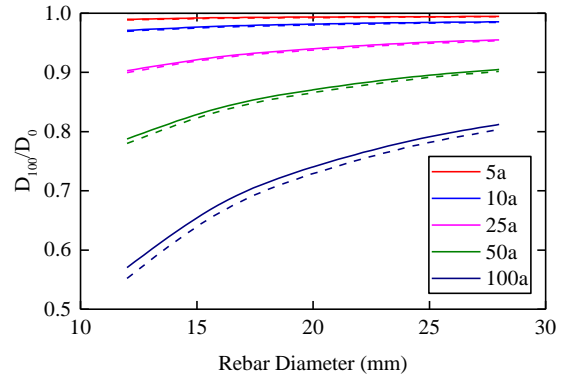


(b) Rebar on center of bottom side

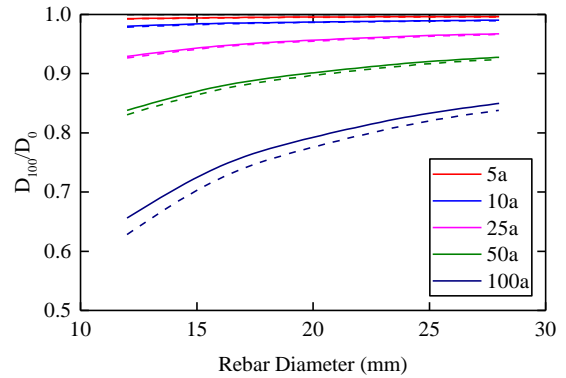
Fig. 20 Mean remaining diameter vs. cover thickness, 16 mm diameter. (Solid-with compensation; Dashed-without compensation;  $D_0$  and  $D_{100}$  denote remaining rebar diameter at initiation and 100a respectively)

microscopic corrosion reaction. Thus a single mean chloride content for each time step was calculated as the attacking chloride content for rebar and mean corrosion depth of rebar was calculated by Liu's model (23). For all FEM models for diffusion space of concrete, chloride content at the nodes on surface of rebar were extracted and their mean value was calculated. Pitting of rebar was neglected. For the analysis of corrosion, temperature  $T=293$  K was adopted in simplification. A generally adopted value of concrete resistance  $R=1500\Omega$  was adopted.

Fig. 20 (cover thickness) and Fig. 21 (rebar diameter) showed corrosion process and characteristics of rebar based on obtained distribution of chloride content around rebar according to the corrosion model in (23) and (24). Ordinate in these figures indicated the ratio of diameter of corroded rebar at 100a to initial value. It has to be noted that corrosion current of rebar is positively correlated with surrounding chloride content. Thus obtained result of rebar corrosion showed less corrosion in the cases with compensation, which was due to larger space for chloride diffusion and lower distributed chloride content. The longer exposure period was, the discrepancy of compensation model (solid) comparing to the case without compensation (dashed) was. Similar results were observed for difference of corner rebar and rebar on center of bottom side compared with the result of distribution of chloride content. Moreover, increasing cover thickness benefited protecting rebar from



(a) Corner rebar



(b) Rebar on center of bottom side

Fig. 21 Mean remaining diameter vs. rebar diameter, 50mm cover. (Solid-with compensation; Dashed-without compensation;  $D_0$  and  $D_{100}$  denote remaining rebar diameter at initiation and 100a respectively)

corrosion. Increasing diameter of rebar extended the service life of rebar. Finally, corner rebar was more dangerous than rebar on center of bottom due to the difference of boundary condition.

## 5. Conclusions

This paper presented a study on the approach of multiscale modeling for diffusion of chloride ion within concrete combining mesoscale and macroscale simultaneously. A three-phase integrated model including core part, compensation part and interfacial transition layer was introduced and discussed in analytical deduction and numerical simulation. Based on the idea of multiscale modeling, two-dimensional mixed model including mesoscopic core part and macroscopic compensation part was created. Cases considering multiscale and single-scale were studied for obtaining chloride content profile of each case. Moreover, corrosion of rebar on corner and straight edge were discussed by means of the multiscale approach. The conclusions of this study are summarized as follows:

- The multiscale approach based on the theory of compensation for mesoscopic numerical simulation of chloride diffusion within concrete introduced in this paper was testified by means of analytical deduction and numerical simulation. The presented work provided the

basis for future large-scale structural durability analysis in optimized size, number of DOFs and time consumption.

- The numerical diffusion analysis was performed within the framework of the two-dimensional mixed model. The proposed approach was verified by comparing the in-site measured data from the literature. Comparison of four types of models indicated computing loading of mixed model was optimized due to much less number of elements and DOFs and meanwhile accuracy was acceptable.
- Effect of compensation on distribution of chloride and corrosion process of rebar were compared in the presented work. Result showed significant difference on distribution of chloride content and rebar corrosion between mixed model and the core model without compensation. Result also related to the configuration of rebar placement, rebar diameter, concrete cover and exposure period. Due to larger space for chloride diffusion and lower distributed chloride content in the cases with compensation, less corrosion of rebar was found by numerical simulation. Exposure period increased the difference of compensation model and the case without compensation.

## Acknowledgements

This paper was sponsored by Project (51508053) supported by the National Natural Science Foundation of China and Project (106112014CDJZR200016) support by the Fundamental Research Funds for the Central Universities, which were greatly appreciated by the authors.

## Reference

- Andrade, C., Alonso, C. and Molina, F.J. (1993), "Cover cracking as a function of bar corrosion: Part I-Experimental test", *Mater. Struct.*, **26**(8), 453-464.
- Angst, U., Elsener, B., Larsen, C.K. and Vennesland, Ø. (2009), "Critical chloride content in reinforced concrete-A review", *Cement Concrete Res.*, **39**(12), 1122-1138.
- Biondini, F., Bontempi, F., Frangopol, D.M. and Malerba, P.G. (2004), "Cellular automata approach to durability analysis of concrete structures in aggressive environments", *J. Struct. Eng.*, **130**(11), 1724-1737.
- Chen, L., Qian, Z. and Wang, J. (2016), "Multiscale numerical modeling of steel bridge deck pavements considering vehicle-pavement interaction", *Int. J. Geomech.*, **16**(1), B4015002.
- Chun Qing, L. (2000), "Corrosion initiation of reinforcing steel in concrete under natural salt spray and service loading-results and analysis", *Mater. J.*, **97**(6), 690-697.
- Francois, R. and Arliguie, G. (1999), "Effect of microcracking and cracking on the development of corrosion in reinforced concrete members", *Mag. Concrete Res.*, **51**(2), 143-150.
- Guo, L., Guo, X.M. and Mi, C.W. (2012), "Multi-scale finite element analysis of chloride diffusion in concrete incorporating paste/aggregate ITZs", *Sci. Chin. Phys. Mech.*, **55**(9), 1696-1702.
- Hiratsuka, Y. and Maekawa, K. (2015), "Multi-scale and Multi-Chemo-Physics analysis applied to fatigue life assessment of strengthened bridge decks", *Computational Plasticity Xiii: Fundamentals and Applications*, 596-607.
- Ladevèze, P. (2004), "Multiscale modelling and computational strategies for composites", *Int. J. Numer. Meth. Eng.*, **60**(1), 233-253.
- Li, J. and Shao, W. (2014), "The effect of chloride binding on the predicted service life of RC pipe piles exposed to marine environments", *Ocean Eng.*, **88**, 55-62.
- Li, X., Wu, F. and Huang, Z. (2009), "Analytical solution to chloride diffusion equation on concrete", *Concrete*, **10**, 30-33. (in Chinese)
- Li, Z., Tu, X. and Chen, A.R. (2014), "Stochastic durability assessment of concrete pylon for long-span cable stayed bridge", *Bridge Maintenance, Safety, Management and Life Extension*, CRC Press, 2544-2551.
- Liu, T. and Weyers, R.W. (1998), "Modeling the dynamic corrosion process in chloride contaminated concrete structures", *Cement Concrete Res.*, **28**(3), 365-379.
- Maekawa, K., Ishida, T. and Kishi, T. (2003), "Multi-scale modeling of concrete performance integrated material and structural mechanics", *J. Adv. Concrete Technol.*, **1**(2), 91-126.
- Maekawa, K., Ishida, T. and Kishi, T. (2009), *Multi Scale Modeling of Structural Concrete*, Taylor & Francis, Inc.
- Mangat, P.S. and Molloy, B.T. (1994), "Prediction of long-term chloride concentration in concrete", *Mater. Struct.*, **27**(6), 338-346.
- Moodi, F., Ramezani-pour, A. and Jahangiri, E. (2014), "Assessment of some parameters of corrosion initiation prediction of reinforced concrete in marine environments", *Comput. Concrete*, **13**(1), 71-82.
- Pan, Z., Chen, A. and Ruan, X. (2015), "Spatial variability of chloride and its influence on thickness of concrete cover: A two-dimensional mesoscopic numerical research", *Eng. Struct.*, **95**, 154-169.
- Pritpal, S.M. and Mahmoud, S.E. (1999), "Flexural strength of concrete beams with corroding reinforcement", *Struct. J.*, **96**(1), 149-158.
- Roberge, P.R. (2008), *Corrosion Engineering Principles and Practice*, McGraw-Hill Education.
- Šavija, B., Luković, M., Pacheco, J. and Schlangen, E. (2013), "Cracking of the concrete cover due to reinforcement corrosion: A two-dimensional lattice model study", *Constr. Build. Mater.*, **44**, 626-638.
- Sun, B., Wang, X. and Li, Z. (2015), "Meso-scale image-based modeling of reinforced concrete and adaptive multi-scale analyses on damage evolution in concrete structures", *Comput. Mater. Sci.*, **110**, 39-53.
- Sun, G., Sun, W., Zhang, Y. and Liu, Z. (2012), "Multi-scale modeling of the effective chloride ion diffusion coefficient in cement-based composite materials", *J. Wuhan Univ. Technol., Mater. Sci. Ed.*, **27**(2), 364-373.
- Torres-Acosta, A.A., Navarro-Gutierrez, S. and Terán-Guillén, J. (2007), "Residual flexure capacity of corroded reinforced concrete beams", *Eng. Struct.*, **29**(6), 1145-1152.
- Torres-Acosta Andrés, A. and Martínez-Madrid, M. (2003), "Residual life of corroding reinforced concrete structures in marine environment", *J. Mater. Civil Eng.*, **15**(4), 344-353.
- Unger, J.F. and Eckardt, S. (2011), "Multiscale modeling of concrete", *Arch. Comput. Meth. Eng.*, **18**(3), 341.
- Vidal, T., Castel, A. and François, R. (2004), "Analyzing crack width to predict corrosion in reinforced concrete", *Cement Concrete Res.*, **34**(1), 165-174.
- Vidal, T., Castel, A. and François, R. (2007), "Corrosion process and structural performance of a 17 year old reinforced concrete beam stored in chloride environment", *Cement Concrete Res.*, **37**(11), 1551-1561.
- Ye, H.L., Jin, X.Y., Chen, W., Fu, C.Q. and Jin, N.G. (2016),

- “Prediction of chloride binding isotherms for blended cements”, *Comput. Concrete*, **17**(5), 665-682.
- Yuan, Q., Shi, C., De Schutter, G., Audenaert, K. and Deng, D. (2009), “Chloride binding of cement-based materials subjected to external chloride environment-A review”, *Constr. Build. Mater.*, **23**(1), 1-13.
- Zhang, R., Castel, A. and François, R. (2009), “The corrosion pattern of reinforcement and its influence on serviceability of reinforced concrete members in chloride environment”, *Cement Concrete Res.*, **39**(11), 1077-1086.
- Zhang, R., Castel, A. and François, R. (2010), “Concrete cover cracking with reinforcement corrosion of RC beam during chloride-induced corrosion process”, *Cement Concrete Res.*, **40**(3), 415-425.
- Zhao, Y., Gao, X., Xu, C. and Jin, W. (2009), “Concrete surface chloride ion concentration varying with seasons in marine environment (Chinese)”, *J. Zhejiang Univ. (Eng. Sci.)*, **43**(11), 2120-2124.
- Zhu, W., François, R., Fang, Q. and Zhang, D. (2016), “Influence of long-term chloride diffusion in concrete and the resulting corrosion of reinforcement on the serviceability of RC beams”, *Cement Concrete Compos.*, **71**, 144-152.